

# Spatially Resolved Galaxy Star Formation and its Environmental Dependence II. Effect of the Morphology-Density Relation

Niraj Welikala<sup>1</sup>, Andrew J. Connolly<sup>2</sup>, Andrew M. Hopkins<sup>3</sup>, Ryan Scranton<sup>4</sup>

## ABSTRACT

In this second of a series of papers on spatially resolved star formation, we investigate the impact of the density-morphology relation of galaxies on the spatial variation of star formation (SF) and its dependence on environment. We find that while a density-morphology relation is present for the sample, it cannot solely explain the observed suppression of SF in galaxies in high-density environments. We also find that early-type and late-type galaxies exhibit distinct radial star formation rate (SFR) distributions, with early-types having a SFR distribution that extends further relative to the galaxy scale length, compared to late-types at all densities. We find that a suppression of SF in the highest density environments is found in the highest star forming galaxies for both galaxy types. This suppression occurs in the innermost regions in late-types ( $r \leq 0.125$  Petrosian radii), and further out in radius in early-types ( $0.125 < r \leq 0.25$  Petrosian radii). When the full sample is considered no clear suppression of SF is detected, indicating that the environmental trends are driven only by the highest SF galaxies. We demonstrate that the density-morphology relation alone cannot account for the suppression of SF in the highest density environments. This points to an environmentally-governed evolutionary mechanism that affects the SF in the innermost regions in both early and late-type galaxies. We suggest that this is a natural consequence of the “downsizing” of SF in galaxies.

*Subject headings:* galaxies: structure — galaxies: statistics — galaxies: distances and redshifts — galaxies: evolution — galaxies: formation

---

<sup>1</sup>Laboratoire d’Astrophysique de Marseille, 38 Rue Frédérique Joliot-Curie, 13388 Marseille Cedex 13, France, niraj.welikala@oamp.fr

<sup>2</sup>Department of Astronomy, University of Washington, Box 351580, Seattle, WA 98195-1580, USA, ajc@astro.washington.edu

<sup>3</sup>Anglo-Australian Observatory, P.O. Box 296, Epping, NSW 1710, Australia, ahopkins@aao.gov.au

<sup>4</sup>Department of Physics, University of California at Davis, One Shields Avenue, Davis, CA 95616-8677, USA

## 1. Introduction

The morphology of a galaxy is an indicator of its internal structure and of the dynamical processes that give rise to it. Edwin Hubble first classified galaxies according to their morphology along the so-called ‘Tuning-fork diagram’ (Hubble 1936; Sandage 1961). Some of the more common classifications are based on visually determining the galaxy morphologies, (de Vaucouleurs et al. 1991; Lintott et al. 2008), while there have been many attempts over the past decade at quantifying morphology using measurements of concentration, color, surface brightness profiles or features in the galaxy spectrum (Abraham, van den Bergh & Nair 2003; Conselice 2006; Goto et al. 2003; Strateva et al. 2001). Broadly speaking, galaxies classified as “early-type” have morphologies that are typically elliptical and lenticular while “late-type” morphologies are either spiral or irregular. Early-types also tend to be redder, more luminous, more gas-poor and have older stellar populations than do late-types.

In dense environments the galaxy population is dominated by early-types. This was first established by Dressler (1980) who studied 55 nearby, rich clusters and found that the S0 fraction increases steadily and the elliptical galaxy fraction increases sharply at the highest densities while the fraction of spiral galaxies decreases steadily with increasing local galaxy density in all clusters. This density-morphology relation implies that the morphology of the galaxy is shaped by the physical mechanisms that are prevalent in that particular environment. The density-morphology relation was also observed in groups of galaxies. Postman et al. (1984), looking at the same dataset found that the relation extended to galaxy group environments identified in the CfA Redshift Survey. The relation is also observed in X-ray selected poor groups (Tran et al. 2001). However Whitmore et al. (1995) found that the relation is very weak or non-existent in groups.

More recently, Goto et al. (2003) studied the density-morphology relation and the morphology-cluster-centric-radius relation in galaxies in the Sloan Digital Sky Survey (SDSS) and found that the elliptical fraction increases and the disc fraction decreases towards increasing galaxy density. They also found that there are two characteristic changes in both relations, suggesting that two different mechanisms are responsible for the relations. In the sparsest regions, they found that both relations became less noticeable, but in the intermediate-density regions, they found that the fraction of S0s increases in higher density environments, whereas the disc fraction decreases. In the densest regions, the S0 fraction decreases rapidly and the elliptical fraction increases, suggesting that a second mechanism is responsible for any morphological transformation of galaxies in the cluster cores. Park et al. (2007), using SDSS galaxies, found that the fraction of early-type galaxies is a monotonically increasing function of local galaxy density and luminosity.

The density-morphology relation has also been detected at higher redshifts. Dressler

(1997) found a strong relation for centrally concentrated clusters at  $z \approx 1$  but not for less concentrated ones. Fasno et al. (2000) studied nine clusters in the redshift range  $0.1 \leq z \leq 0.25$  and found a density-morphology relation in high elliptical concentration clusters though not in low elliptical concentration clusters, consistent with Dressler (1997). They also traced the morphological fraction as a function of cosmic time and, confirming the “Butcher-Oemler effect” (Butcher & Oemler 1978), found that the S0 fraction decreases with increasing redshift while the spiral fraction increases. However, Holden et al. (2007), using galaxies in five massive X-ray clusters from  $z = 0.023$  to  $z = 0.83$  found that the evolution of the morphology-density relation differs considerably between galaxies selected by stellar mass and those selected by luminosity, the early-type fraction changing much less in mass-selected samples. The result is echoed by van der Wel et al. (2007) who used galaxies in the SDSS and the GOODS-South field and found little change in the morphology-density relation since  $z \approx 0.8$  for galaxies more massive than  $0.5 M_{\star}$ .

The same physical mechanisms that are proposed to explain the relation between SFR and environment have been proposed to explain the morphology-density relation as well. These include ram pressure stripping of gas (Gunn & Gott 1972), gravitational interactions between galaxies (Byrd & Valtonen 1990), galaxy harassment via high-speed encounters (Moore 1996) and galaxy mergers. However, little observational evidence exists to suggest that these processes drive the evolution in galaxies. On the theoretical front, the combination of semi-analytic models with N-body simulations of cluster formation has enabled the density-morphology relation to be simulated. Diaferio (2001) derived the relation assuming that galaxy morphologies (determined in the simulation using a bulge-to-disc ratio) in clusters are solely determined by their merging histories. They found good agreement with data from the CNOC1 sample (Yee et al. 1996) for bulge-dominated galaxies. Benson et al. (2001) found that a strong density-morphology relation was established at  $z = 1$  which was similar to that at  $z = 0$  but their results suggested that more than one of the physical mechanisms mentioned above may have to be used to explain the relation.

In Welikala et al. (2008) (hereafter Paper I), we studied the spatial variation of SF within galaxies as a function of the galaxy environment, for 44,964 galaxies in the SDSS. We showed that the star formation rate (SFR) in galaxies in high-density regions is suppressed compared to those in lower-density regions. We showed that this suppression occurs in the innermost regions within galaxies ( $r \leq 0.25R_p$  where  $R_p$  is the Petrosian radius). The study dealt with galaxies of all morphologies. We now aim to extend that investigation by focusing on the following three questions:

1. Do early-type and late-type galaxies, which have distinct radial light profiles, also have distinct radial distributions of SF? This may be associated with different formation

mechanisms or evolutionary histories in either galaxy type.

2. Does any type-dependent change in the spatial distribution of SFR occur for all galaxies of that type uniformly? Or is it restricted to a sub-population, such as the highly star forming systems? In Paper I we established that the suppression of SF seen in high density environments for the full sample is a consequence of suppression only in the highly star forming sub-population. We want to establish whether the trends in early and late type galaxies separately are also dominated by this active sub-population.
3. Is the observed environmental dependence of SFR in galaxies a consequence of, or in addition to, the reduced average SFRs expected simply from the higher proportion of early-types in high density environments?

We describe our method and approach in §2, and our results in §3. These are discussed in §4, where we explore an evolutionary explanation for the observed trends. We present our conclusions in §6. We assume throughout that  $\Omega_\Lambda = 0.7$ ,  $\Omega_M = 0.3$ , and  $H_0 = 75 \text{ km s}^{-1} \text{ Mpc}^{-1}$ .

## 2. Method

### 2.1. The Pixel-z and Environmental Measures

In Paper I we determined the radial variation of SF in 44,964 galaxies in the Fourth Data Release (DR4, Adelman-McCarthy et al. (2006)) of the Sloan Digital Sky Survey (SDSS, York et al. (2000)) using a technique called ‘pixel-z’ (Welikala et al. 2008; Conti et al. 2003). This technique involves fitting spectral energy distributions (SEDs) generated from the stellar population synthesis models of Bruzual & Charlot (2003) to the photometric fluxes in five bands ( $u, g, r, i, z$ ) in individual pixels of each galaxy (see Paper I for details). The calculation of the fluxes in each pixel of every galaxy image is described in Appendix A. The SFR in each pixel is calculated directly from the best fit SED to the pixel fluxes and an associated uncertainty from that fit is also calculated.

Given the SFR determined for every pixel in every galaxy, we determined both the total SFR in each galaxy and the spatial variation of SF within galaxies in the sample. We used this to explore the environmental dependence of the radial variation of SFR in galaxies. We found that the suppression of total SFR in galaxies in high density regions is an effect seen most strongly in the high-SF population and is a consequence of centrally suppressed SF.

In the current analysis we use the same galaxies in DR4, the same environmental measure

based on the spherical density estimator, and the same pixel-z estimates for SFR as in Paper I. We retain the same two morphological classes as in Paper I, as used also by Goto et al. (2003), based on discriminating galaxies according to their inverse concentration index  $C_{in}$  which is found to be correlated with the galaxy type (Shimasaku et al. 2001; Strateva et al. 2001). We use  $C_{in}$  to classify galaxies into two broad morphological classes: early-types (E,S0,Sa) and late-types (Sb, Sc and Irr).  $C_{in}$  is defined as the ratio of the radius containing 50% of the Petrosian flux (`petroR50_r`) to the radius containing 90% of the Petrosian flux in the galaxy (`petroR90_r`). `petroR50_r` and `petroR90_r` are obtained from the `PhotoObjAll` table in the Catalog Archive Server (CAS) in DR4<sup>5</sup>. A descriptions of how the Petrosian flux is calculated is given in Blanton et al. (2001). The selection results in 27 993 early-type galaxies ( $C_{in} \leq 0.4$ ) and 16 971 late-type galaxies ( $C_{in} > 0.4$ ) classified according to this parameter.

To establish that our results are not sensitive to, or biased by, this choice of morphology proxy, we duplicate our analysis using the Sersic index. The Sersic model for the surface brightness in a galaxy is given by  $I(r) = I_0 e^{(-r/r_0)^{1/n}}$ , where  $I(r)$  is the intensity at an angular radius  $r$ ,  $I_0$  is the central intensity,  $r_0$  is the characteristic radius, and  $n$  the Sersic index or profile shape parameter. An exponential profile is recovered with  $n = 1$ , while  $n = 4$  gives the traditional de Vaucouleurs profile. The Sersic indices for the galaxies are found by cross-matching galaxies in our sample with those found in the NYU Value Added Galaxy Catalog (NYU-VAGC<sup>6</sup> and Blanton et al. (2005)) where the Sersic profiles for the galaxies are made available. The Sersic profiles are stored in the `sersic_catalog.fits` files and the values of  $n$  for the objects are stored in the column `SERSIC_N[i]` where  $i$  denotes a particular passband. Unlike concentration, the Sersic indices have been corrected for the effects of seeing. In our analysis we classify galaxies with  $n < 2$  as late-types and those with  $n > 2$  as early-types.

We first investigate the effect of an improved method to obtain the total SFRs in galaxies, based on the method for obtaining the mean radial SFR.

## 2.2. The Total Galaxy SFR-Density Relation: An Improved Estimate

In Paper I, we investigated how the distribution of galaxy SFRs changes as a function of the local (spherical) galaxy density. The SFR due to stellar populations within each pixel

---

<sup>5</sup><http://cas.sdss.org/dr4/en/>

<sup>6</sup><http://sdss.physics.nyu.edu/vagc>

of a galaxy is assumed to follow an exponential functional form  $\Psi(t) = \Psi_0 e^{(-t/\tau)}$ . In Paper I, the total SFR for each galaxy was calculated from the weighted sum of the SFRs in each pixel in the galaxy image, where the weights correspond to the reciprocal of the square of the fractional error on the SFR in each pixel. The weighting is done to avoid giving undue significance to poorly constrained pixels, such as pixels dominated by the sky background, so that these pixels do not bias our measurements.

In the estimation of the radial variation of mean SFR within galaxies, we performed a weighted mean of SFRs of the pixels within each radial annulus of each galaxy, out to  $r=1.5$  Petrosian radii ( $1.5R_p$ ) in the  $r'$  band. Here, in calculating the total SFR, we also limit the spatial extent within which the SFR in the pixels is counted. The total SFR for each galaxy is therefore calculated from the sum of SFRs in all pixels in the galaxy, summed within consecutive radial annuli from the center of the galaxy up to  $1.5R_p$ . We find that estimating the total SFR within  $1.5R_p$  captures the vast majority of high signal-to-noise pixels that actually belong to the galaxy while not including the contribution of very low signal-to-noise pixels in the outskirts of the galaxy. While low surface brightness, low signal-to-noise pixels in the galaxy outskirts should individually have only a very small contribution to the total SFR (since we are weighting the SFR in each pixel by the square of the signal-to-noise), galaxies can have a substantially large areas of these low signal-to-noise pixels which extend well beyond the disk scale length. The combined contribution of these pixels could therefore bias the total SFR that is calculated. This appears to be less of a problem for typical disk galaxies than for bulge-dominated systems which can have a large area of these low-surface brightness pixels surrounding the galaxy. The second motivation of reducing the spatial extent is to remove a secondary contaminant: a smaller number of pixels which extend even beyond  $2R_p$  of the galaxy and are clearly sky pixels whose fluxes are still fitted by the algorithm. Limiting the spatial extent to  $1.5R_p$  within which the SFR in the pixels is counted, as was done in the radial analysis, therefore provides a more accurate estimate of the total SFR in the galaxy.

Figure 1 shows the variation of the total SFR distribution with local density for the full sample of galaxies (all types) and for the early-type and late-type subsamples within this. The three lines in each plot correspond to the 25th, median and 75th percentiles of the SFR distribution. Removing a larger component of the low signal-to-noise pixels results in a more marked separation between the SFR distributions of early and late-type galaxies at all densities. Late-type galaxies now dominate the tail of the total SFR distribution – they are seen to be more highly star-forming than early-types at all densities. The trends with environment are the same as the ones found in Paper I, Figure 9. It can be seen that in all three samples, the total SFR in galaxies is still correlated with the local environment as was found by Lewis et al. (2002) and Gómez et al. (2003). As stated in Paper I, the

fluctuations at low densities are characteristic of the size of the systematic uncertainties in these measurement. In all three samples, the SFR decreases with increasing density, with the greatest effect in the highest density environments:  $> 0.05 (h^{-1} Mpc)^{-3}$  for early-types and for the full sample and  $> 0.055 (h^{-1} Mpc)^{-3}$  for late-types (these densities correspond to the outskirts of rich clusters). In each of the three samples, the effect is most noticeable in the most strongly star-forming galaxies, i.e. those in the 75th percentile of the SFR distribution. The SFR distributions in all three samples are skewed towards higher SFRs at low densities. As density increases, the skewness of the SFR distributions in the early and late-type galaxies decreases. It is also worth noting that even in the highest density environments, the SFR of these high-SF late-type galaxies is higher than for the early-types.

Limiting the spatial extent to  $1.5R_p$  over which the total SFR in galaxies is estimated, as well as performing a weighted sum over the pixels, thus removes a source of contamination that was more significant than previously thought. This results in a clearer separation between early and late-type galaxies in terms of the total SFR distribution. The trends between SFR and environment, however, remain largely intact.

### 3. Radial and environmental trends in SFR

#### 3.1. The Density-Morphology Relation

Figure 2 illustrates the density-morphology relation in this sample of SDSS galaxies. The proportion of early-type galaxies, with  $C_{in} < 0.4$ , is shown to be increasing as a function of local galaxy density. In the low-density environments around 50 percent of galaxies are early-types, while in the highest density environments this increases to around 75 percent. The bottom panel gives the total number of galaxies found in each density interval. These plots sample the local galaxy density more finely than in the analysis of Paper I, or in subsequent analyses herein where only three intervals of local density are used. We use the results of the density-morphology relation below in § 3.4 when assessing whether the observed suppression in SF can be recovered simply by mimicking this effect. Before we can do this, though, we need to establish the radial variation of SFR for each morphological type as a function of environment.

#### 3.2. Radial Variation of SFR as a Function of Environment

Here we examine the radial distribution of SFR in both early-type and late-type galaxies as a function of their environment for galaxies (a) spanning the entire range of (total) SFR

and (b) within the highly star-forming population only.

We calculate the weighted mean SFR  $\psi_w$  for each radial annulus in every galaxy (see Paper I for details). For a sample of galaxies this gives a distribution of  $\psi_w$  for each annulus. Figure 3 shows the 75th percentile of  $\psi_w$  for the early-types, late-types and for the full sample, within three intervals of galaxy density (corresponding to the three panels in the Figure). As shown in Paper I the effect of environment is most pronounced for the 75th percentile of  $\psi_w$ , rather than the median of  $\psi_w$ . In determining the radial variation of SFR and its dependence on environment we focus on the 75th percentile of  $\psi_w$  in this study.

*Both early and late-type galaxies have distinct radial SFR profiles.* This answers the first of the questions we posed above. The peak of  $\psi_w$  in early-types is significantly lower than in late-type galaxies. The SF in the center is very low, reflecting the fact that in early-type systems, which are typically bulge-dominated, the stellar populations in the center of the bulge are old and there is consequently little ongoing SF. In contrast, the stellar populations with higher SFR are further out in the bulge and the mean SF in this region is also better sampled. The early-type galaxies show a more extended distribution of SF which peaks further out in radius than in late-type galaxies. This reflects the fact that late-type galaxies have a smaller bulge compared to early-types.

In the late-types most of the SF takes places in the inner part of the disk, closer to the center. There is thus a very sharp increase in SFR as we go from the center ( $r \leq 0.125 R_p$ ) to the inner part of the disk ( $r \approx 0.25 R_p$ ) followed by a rapid decline in the SFR throughout the disk to the outskirts. Disk galaxies have, on average, a much higher SFR up to  $r \approx 0.25 R_p$  (by as much as  $0.014 M_\odot \text{ yr}^{-1}$  in the lowest density environments and  $0.012 M_\odot \text{ yr}^{-1}$  in the highest density environments) than do the early-types. This reflects the younger star-forming stellar populations in the disks of these galaxies.

As described in Paper I, the effect of galaxy density on the full sample (all types) is to cause a suppression of SF in the centers of galaxies ( $r < 0.25 R_p$ ) while no effect is observed for  $r > 0.25 R_p$ . Figure 3 also shows that the effect of the environment on the full sample of galaxies (early and late types together, green curve) is to push the peak of the SFR profile to larger radii. However, Figure 3 also shows that when galaxies in the full sample are divided by type, the SFR radial profiles of early and late-type galaxies do not change significantly across the different environmental ranges.

A straightforward explanation of the trend in the full sample in terms of the density-morphology relation presents itself, namely that at low densities there is almost an equal fraction of early and late-type galaxies, while at higher densities the profile is progressively more dominated by the higher contribution from early-types. It is important to note that



while the shifting of the peak mean SFR in the full sample of galaxies may indeed be explained simply by the increasing fraction of early-type galaxies in higher density environments, there are other aspects of the density dependence that are not.

### 3.3. The Significance of Highly Star Forming Galaxies

In Paper I it was found that the most significant decrease in the total SFR with increasing local galaxy density takes place for galaxies in the top quartile of the total SFR distribution. Here we explore the radial SFR profiles for the galaxies that are in the top and second quartile of the total SFR distribution for each galaxy type, to identify whether the trends with environment are driven only by the most active star-forming galaxies. In §3.5, we also examine the proposal by Park et al. (2007) that the trends are instead driven primarily by the most luminous galaxies.

We refer to the top quartile of the total SFR distribution, for both morphological types, as the “highest SF galaxies,” and the second quartile as the “the next highest SF galaxies”. We examine the distribution of  $\psi_w$  for these subpopulations for early and late-types separately, determining the quartiles of  $\psi_w$  of these distributions as above in the same intervals of local galaxy density. The results, as before, are most prominent in the 75th percentile of  $\psi_w$  (compared to the median or 25th percentile) and radial trends for only this quartile are shown.

The results of this analysis are presented in Figure 4, with the full sample spanning all SFRs shown for comparison in Figure 5. Figure 4 shows the 75th percentile of  $\psi_w$  for the highest and next highest SF galaxies for both galaxy types. In the early-type highest-SF galaxies there is a relatively small suppression ( $1.5\sigma$ ) in  $\psi_w$  between the least and most dense environments but only in the region  $0.125 < r/R_p \leq 0.25$ . We do not see a significant effect of environment on the SFR in early-types in the center ( $0.0 < r/R_p \leq 0.25$ ) or in the outskirts. In the next highest SF early-types, we do not detect a similar suppression in the SF, suggesting that this is a phenomenon that affects only the most active early-type systems. In the highest-SF late-type galaxies, we detect a suppression of  $3\sigma$  in the mean SFR in the center ( $r/R_p \leq 0.125$ ), while there is no significant suppression of SF at other radii. In the next highest SF late-types, we find a slightly lower suppression in  $\psi_w$  of  $2\sigma$  in the SFR in the center ( $r/R_p \leq 0.125$ ), and again, no significant effect of the environment at other radii. The cores of late-type galaxies thus have their SF reduced in more dense environments, while the SF in the remainder of the disk and outskirts is largely unaffected by a changing environment. Further, unlike the early-type systems, this affects a larger proportion of star-forming late-types. All late-types in the top two quartiles of the total

SFR distribution have their central SFR suppressed in the highest densities. In contrast, in the early-types, we detect a suppression only in galaxies in the highest quartile of the total SFR distribution.

A Kolmogorov-Smirnov (KS) test on the distribution of  $\Psi_w$  of the two innermost annuli in both the lowest density interval ( $0.0 < \rho \leq 0.01 (h^{-1} \text{Mpc})^{-3}$ ) and the highest density interval ( $0.04 < \rho \leq 0.09 (h^{-1} \text{Mpc})^{-3}$ ) rules out the hypothesis that the populations in the two density ranges are derived from the same underlying distribution at more than 99% confidence level. This holds for the full sample of highly star-forming galaxies or for early and late-type galaxies considered separately. The observed suppression of SF in the central regions of these galaxies is therefore an effect of the environment rather than being due to stochastic fluctuations.

Figure 5 shows the results of performing a similar analysis for the full sample of early and late-type galaxies, without making any cuts in total SFR. Neither galaxy type shows any statistically significant variation in the 75th percentile of  $\psi_w$  with environment at any radius when the full sample of galaxies of each type is considered. *The suppression of SF in the highest density environments is therefore driven by the most active, highly SF galaxies.* This answers the second of the questions posed above. It is also worth noting that, as found for the full sample in Paper I when considering both morphological types together, the SFR in the outskirts of either the early or late-type galaxies is not affected by a changing environment. The right-hand panels of Figure 5 also show the radial SFR profiles when the Sersic index is used as a proxy for galaxy morphology. It is clear that these results hold independent of the choice of inverse concentration index  $C_{in}$  or the Sersic index as the morphological proxy.

### 3.4. Can the density-morphology relation alone explain the suppression of star formation?

The results for the high SF populations of either galaxy type suggest that the suppression of SF is not due solely to the density-morphology relation. In order to determine definitively whether the suppression in SF is a result of the density-morphology relation or if another, perhaps evolutionary, mechanism is at work, we carry out a further test. We have determined the radial SFR profiles for the early and late-types in the lowest density environments, together with the fraction of early and late-types as a function of density. So we can now ask how the radial SFR profile compares for the full sample (all types) in the highest density environment with a profile constructed by combining the low-density profiles for each morphological type in the proportions appropriate to the high-density environment.

Let  $\Psi(r, \rho)_E$  be the mean SFR profile of early-types at density  $\rho$ ,  $\Psi(r, \rho)_L$  the mean SFR profile of late-types at density  $\rho$  and  $\Psi(r, \rho)_T$  the mean SFR profile of all types at density  $\rho$ . We will use  $\rho_1$ ,  $\rho_2$ ,  $\rho_3$  to refer to the lowest, intermediate, and highest density environments respectively. Figure 6 shows the radial variation of  $\Psi(r, \rho)_E$  and  $\Psi(r, \rho)_L$ . The high value of the mean, compared to the 75th percentile, reflects an underlying distribution of  $\psi_w$  that is skewed towards higher values of SFR. The trends in the mean reflect many of those observed with the 75th percentile in that there is little effect of environment on the outskirts of the galaxies of either type, but there is a more marked suppression in the mean of  $\Psi$  in the galaxy center in either type. This is true for both the high SF galaxies and for the full sample of early and late-types (the mean being more sensitive to the high SFRs in the most active galaxies). For the high SF late-types, there is a relatively high mean  $\Psi$  in the galaxy center ( $r/R_p \leq 0.125$ ) and this is suppressed by about  $2\sigma$  in the highest density environment  $\rho_3$ . In the high-SF early type galaxies, there is a  $2\sigma$  suppression in the first two inner annuli, up to  $r \leq 0.25R_p$ .

Suppose the suppression of SF is just due to the density-morphology relation, simply a higher fraction of early-types in high-density environments. We can use the individual SF profiles of early and late-type galaxies at low densities  $\rho_1$  to determine what the profile for the composite sample would be at the highest densities  $\rho_3$ . To do this we take  $\Psi(r, \rho_1)$  for early and late-types, explicitly assuming these remain the same within different environments, and average them, weighted by the relative proportion of early and late types at  $\rho = \rho_3$ . This produces an artificial composite profile at  $\rho = \rho_3$  that reflects the profile expected if it arose solely from the density-morphology relation:

$$\Psi(r, \rho_3)_{\text{artificial}} = \frac{N_E}{N_E + N_L}(\rho_3) \times \Psi(r, \rho_1)_E + \frac{N_L}{(N_E + N_L)}(\rho_3) \times \Psi(r, \rho_1)_L. \quad (1)$$

We compare this artificial profile at  $\rho = \rho_3$  to the one actually observed at  $\rho = \rho_3$ :

$$\Psi(r, \rho_3)_{\text{observed}} = \frac{N_E}{N_E + N_L}(\rho_3) \times \Psi(r, \rho_3)_E + \frac{N_L}{(N_E + N_L)}(\rho_3) \times \Psi(r, \rho_3)_L. \quad (2)$$

$\Psi(r, \rho_3)_{\text{observed}}$  is of course simply equal to  $\Psi(r, \rho_3)_T$ .

The result of this composite SFR profile is shown in Figure 7 for both the highest SF galaxies and for the full sample. The observed SFR profile in both cases is significantly below the artificial SFR profile, particularly in the innermost annulus  $r \leq 0.125R_p$ . *This shows directly that the density-morphology relation alone cannot give rise to the observed suppression in SF in centers of galaxies in high density environments.* This answers the third of the questions we initially posed, but raises another. Since the effect is not due to the morphology-density relationship alone, what is the mechanism or mechanisms that drive the

observed suppression in SF? Before addressing this, we briefly investigate the possibility that our results, which are a consequence of the highest SF galaxies, are a simple consequence of higher SFRs in more luminous galaxies.

### 3.5. The Effect of Luminosity

Here we investigate the effect of galaxy luminosity on the radial variation of SF and its dependence on environment. Park et al. (2007) studied the color gradients of galaxies brighter than  $M_r = -18.5$  as a function of the local galaxy density in the SDSS. For early-type galaxies, they found no environmental dependence of the color gradient at a given absolute magnitude, and in addition found that the gradient is almost independent of the luminosity as well. They also found that for late-type galaxies which are bright, there is no dependence of the gradient on environment, while for fainter late-types, there is a weak dependence on environment - fainter galaxies were seen to become bluer at the outskirts (relative to the galaxy center) at low densities while the color gradient vanishes in high density environments. In order to determine if the luminosity of galaxies has some effect on the radial variation of SF and the way it depends on the galaxy environment, we split our galaxies into narrower intervals of absolute magnitude and examine the radial distribution of SF within the early and late-type galaxies in each interval, across the same range of densities. K-corrected absolute magnitudes are obtained from the CMU-Pitt SDSS Value Added Catalog (VAC) database<sup>7</sup>, where the k-corrections had been applied according to Blanton et al. (2003). The top panel of Figure 8 shows the SFR profiles (75th percentile of  $\psi_w$ ) for early-type galaxies in the absolute magnitude intervals  $-22.5 < M_r \leq -21.5$  and  $-21.5 < M_r \leq -20.5$  respectively, and the bottom panel is for the late-type galaxies for the same absolute magnitude intervals. The general characteristics of the profiles for both types remain unchanged when we split our sample into these narrower intervals of luminosity. We detect no effect of the environment on the SF in the brighter sample but do recover the suppression of SF with increasing local density in the fainter sample.

For the brighter early-type galaxies we find no significant change in the variation of SF with galaxy density in either the center or outskirts of the galaxies, which is consistent with the findings of Park et al. (2007). But for the fainter early-type galaxies we do detect a suppression of SF at higher densities. There is a decrease of  $2.5\sigma$  in  $0.125 < r/R_p \leq 0.25$  between the lowest and highest local density intervals, while there is no change in the SFR with increasing density in the outskirts.

---

<sup>7</sup><http://nvogre.phyast.pitt.edu/dr4/>

For the late-type galaxies, just as for the early-types, there is no change in the mean SFR at any radius with environment for the brighter sample, which is consistent with the Park et al. (2007) result. For the fainter sample, there is a decrease in the mean SFR (approximately a  $2\sigma$  difference) in the region  $r/R_p \leq 0.125$ , while the mean SF in the outskirts is again unchanged. Park et al. (2007), however, finds that at the highest densities, both the center and the outskirts become redder (giving zero color gradient).

There are some conclusions to be drawn here. First, there is no indication that our primary results are a direct consequence of a SFR-luminosity relation, since it is the fainter subsample that contributes primarily to the trends with environment that are observed. There remains the caveat that the sample selection was very different between the two groups: Park et al. (2007) classified galaxies based on their locations in the  $u-r$  versus  $g-i$  color gradient space as well as concentration index space (Park & Choi 2005) whereas we use concentration alone. Also, degeneracies, such as that between age and metallicity, may contribute to the difference between our result and that of Park & Choi (2005). Finally, the disparity between the two sets of results may also be explained to some extent by the inclusion of dust obscuration in the pixel- $z$  analysis. SFR gradients may be observed in the absence of color gradients, as the effect of dust will be to redden otherwise bluer star forming stellar populations.

#### 4. Discussion

The distinct radial SF profiles separate the two galaxy types cleanly. Early-types have a lower mean SFR throughout compared to late-type galaxies. The environment is found to affect the highest SF early-type galaxies only while affecting the late-type galaxies in both the highest and second highest quartiles of their total SFR distribution. In the highest SF early-type galaxies, the suppression of SF takes place in  $0.125 < r/R_p \leq 0.25$  while in the the late-type galaxies, the suppression takes place at  $r/R_p \leq 0.125$ . This suggests that the suppression in SF in these active galaxies of either type, is independent of the established density-morphology relation.

It is worth noting that, as found for the full sample in Paper I, the outskirts of galaxies in either the early or late-type galaxies are not affected by a changing environment. This implies that the outskirts of either type of galaxy are not significantly affected by processes such as ram-pressure stripping and galaxy harassment or interaction between galaxies, processes which remove cold gas available for star formation, and which should primarily affect the outskirts of galaxies before they affect the inner regions. The lack of effect in the outskirts could alternatively be due to the fact that these processes affect only a small fraction of

the population. Our results are consistent with the conclusions of Cooper et al. (2006) who studied the relationship between galaxy properties and environment at  $0.75 < z < 1.35$  in the DEEP2 Galaxy Redshift Survey. Their findings suggest that cluster-specific processes, such as ram-pressure stripping and harassment, are not needed to establish the color-density relation and that the group environment too plays a critical role in quenching star formation. A similar result is echoed at low and intermediate redshifts (van den Bosch et al. 2008; Patel et al. 2008).

The short timescales for the physical mechanisms of SFR quenching would also make them difficult for our method to detect as they will only be detectable for a small fraction of the sample at any given redshift, and this will be hidden by our quartile sampling statistics. This is supported by the results of Doyle & Drinkwater (2006), who find a reduction in the *number* of galaxies with neutral hydrogen (HI) in high-density environments, but no significant trend with environment in the star formation rate or efficiency of star formation in HI galaxies. There is also the possibility that some of these processes could be taking place at much lower densities than we are probing.

The results of §3.4 suggest that the suppression of SF cannot be due to the density-morphology relation alone. Given that both physical “infall and quench” mechanisms and the density-morphology relation are ruled out as the main mechanisms of SF suppression in either type of galaxy, we explain the trends observed by extending the “downsizing of SF” hypothesis laid out in Paper I in terms of galaxy morphology.

Downsizing is characterized by a decrease in the mass of galaxies that dominate the SFR density with increasing cosmic time. This was first suggested by Cowie et al. (1996) who found that the maximum rest-frame K-band luminosity of galaxies undergoing rapid star formation has been decreasing smoothly with time in the redshift range  $z = 0.2 - 1.7$ . This is supported by more recent studies of star-formation histories of galaxies in both the local and distant universe. Heavens et al. (2004) observed that the most massive local galaxies seen in the SDSS also appear to be dominated by stars which formed at early epochs. Juneau et al. (2005) studied the cosmic SFR and its dependence on galaxy stellar mass in galaxies in the Gemini Deep Deep Survey (GDDS) and found that the SFR in the most massive galaxies ( $M_\star > 10^{10.8} M_\odot$ ) was 6 times higher at  $z = 2$  than at present and that the SFR at  $z = 2$  falls sharply to reach its present ( $z = 0$ ) value by  $z \approx 1$ . Panter et al. (2004) found no evolution in the stellar mass function of galaxies in the SDSS in the redshift range  $0.05 \leq z \leq 0.34$  indicating that almost all stars were formed by  $z \approx 0.34$  with little SF activity since then. In a radio-selected survey, Seymour et al. (2008) also determined that high mass galaxies only contribute significantly to the SFR density of the universe at high redshifts, with low-mass systems dominating at lower redshift.

To interpret our results we consider a population of galaxies that is active and highly star forming at high redshifts. These will ultimately form early-type galaxies and include in particular the most massive systems that form within the more massive dark-matter halos in dense environments. As the SF, in the “downsizing” scenario, is progressively associated with less massive galaxies in lower-mass halos and less dense environments, the SF moves from being dominant in cluster regions at high redshift to being dominant in low-density regions at low redshifts. This explains the density-morphology relation. To explain the radial dependence of SF with environment – the central suppression of SF in the high-SF galaxies – we consider that bulges within late-type galaxies may form and evolve similarly to early-type galaxies (Driver et al. 2007). This will result in late-type galaxies in high-density environments having bulges that formed the bulk of their stars earlier than similar late-types in lower-density environments. These will consequently show the same kind of reduced current SF, purely as a consequence of their rapid early evolution, compared to late-types in lower-density environments. This is also consistent with the observed reduction in the SFR of early-types in high-density environments.

A natural consequence of downsizing in galaxies would be that the SFR-density relation should invert at higher redshifts, with increased SFR in the more dense environments. This has been measured by Elbaz et al. (2007) using data from the Great Observatories Origins Deep Survey (GOODS) at  $z \approx 1$ . They found the SFR-density relation observed locally was reversed at  $z \approx 1$ , with the average SFR of galaxies increasing with increasing local density. Cooper et al. (2008), using galaxy samples drawn from the SDSS and the DEEP2 Galaxy Redshift Survey, found an inversion of the SFR-density relation from  $z \approx 1$  to  $z \approx 0$ . They found that this evolution in the SFR-density relation is driven, in part, by a population of bright, blue galaxies in dense environments at  $z \approx 1$  (Cooper et al. 2006). This population is thought to evolve into members of the red sequence from  $z \approx 1$  to  $z \approx 0$ . This adds additional support to the interpretation of our observed SFR suppression at low redshifts in terms of downsizing.

Reproducing the radial SFR profiles and their density dependence may require some addition to current models. It has recently been shown (Neistein et al. 2006) that downsizing could be a natural outcome of hierarchical structure formation if mass assembly and star formation are treated as distinct processes that proceed in opposite directions, and if a characteristic mass for SF truncation is introduced. Stars can form first in the small building blocks of today’s massive galaxies. If gas processes limit galaxy formation to dark matter halos above a minimum mass, a certain downsizing arises naturally from the mass assembly process itself (Neistein et al. 2006). Cattaneo et al. (2008) who studied the origin of downsizing of elliptical galaxies using the mean stellar ages of galaxies, showed that this could result naturally from a shutdown of star formation in dark matter halos above a critical

mass of  $10^{12}M_{\odot}$ . Above this mass there is stable shock heating which truncates the star formation.

Our observations could well be driven by the downsizing of SF together with a treatment of late-type galaxy bulges in a similar fashion to early-type bulges, resulting in the observed central suppression of SF in high density environments. More work needs to be done on the theoretical front, however, if the observed dependence of the radial SF on the environment is to be reproduced in the models.

## 5. Limitations of this analysis

In future work, we would like to perform our analysis with additional morphological proxies. An improvement in the accuracy of the classification using the concentration index  $C_{in}$  alone could potentially be achieved by calculating `petroR50_r` and `petroR90_r` using elliptical rather than circular apertures. This would address the problem of late-type galaxies with small axis ratios (edge-on) being classified as early-types erroneously. This is unlikely to change our statistical results significantly since the random orientation of galaxies in our sample, both on the sky and to the line of sight, will act to mitigate any systematic effects when we average over annuli. This is supported by the results of selecting only face-on and edge-on galaxies of either type in our sample using the axis-ratios given in the CAS and repeating our analysis - the 75th percentiles for  $\Psi$  are found to be invariant to the effect of inclination. More recently, a catalog of visually-classified morphologies of galaxies in the SDSS has become available through the Galaxy Zoo project (Lintott et al. 2008). Since this avoids biases introduced by other morphological proxies such as concentration or color, we would aim to repeat our analysis using this new classification.

The second issue we would like to attempt in future work is to implement a full seeing correction to the colors in the pixels. More than half of the galaxies in our sample have innermost radial annuli ( $r < 0.125R_p$ ) which are larger in angular size than the PSF width. We have chosen a rather coarse grid of stellar population parameters (age, e-folding time, dust obscuration and metallicity). Color corrections due to seeing variability across different passbands are not expected to change the values of the inferred parameters of the stellar populations in the pixels beyond the bounds of the error range that the technique has estimated, although it cannot be ruled out for a small number of pixels where degeneracies between the stellar population parameters are severe. In general, the inferred parameters for these severe cases should be associated with large uncertainties but this may not always be the case. In future work, we will attempt to quantify the effect of these degeneracies and color corrections on the estimated values of the inferred parameters and their associated



uncertainties. Along with this, we also aim to implement a full seeing model for the pixels and a correction for the seeing variability across the various passbands.

## 6. Conclusions

We use the “pixel-z” technique as in Paper I, here dividing SDSS galaxies by morphology in order to study the role of the density-morphology relation on the spatially resolved SF in galaxies. A density-morphology relation is quantified for our volume-limited galaxy sample. We find that a suppression of SF occurs in the most active and highly star-forming systems in the highest density environments for both broad galaxy morphological types. We find that neither “infall and quench” mechanisms nor the density-morphology relation by themselves can account for this observed suppression of SF in either early or late-type galaxies. The results are consistent with the picture of “downsizing” in galaxy formation, together with the idea that late-type galaxy bulges form and evolve in a similar fashion to early-type galaxies, leading to a lower SFR in high-density environments.

In particular, we observe the following:

- Early and late-type galaxies in the SDSS each have a distinct spatial variation of SF, with early types having a SFR distribution that extends further (relative to the galaxy scale length) compared to late-type galaxies.
- A suppression of SF occurs in the most active and highly star-forming systems in the highest density environments for either galaxy type. The suppression takes place in the innermost regions of the galaxies, occurring at  $0.125 < r/R_p \leq 0.25$  for early-type galaxies and  $r/R_p \leq 0.125$  for late-type galaxies.
- In early-type galaxies, only those in the top quartile of the total SFR distribution ( $\text{SFR} > 0.45 M_\odot \text{yr}^{-1}$ ) show any significant SF suppression in cluster environments. In late-type galaxies, there is a much larger range of total SFR in these galaxies (the top two quartiles) where a suppression of SF is observed.
- We find no significant environmental dependence when considering the full sample of early and late-type galaxies, indicating that the trends with environment are driven by the highly star-forming galaxies.
- The suppression of SF is seen primarily in lower-luminosity galaxies ( $-21.5 < M_r \leq -20.5$ ) in our sample, while we detect no environmental dependence on the radial distribution of SF for brighter galaxies.

- By appropriately weighting the average SFR profiles of early and late-type galaxies in low-density regions by the proportions of these types found in high-densities, we show that the density-morphology relation alone cannot account for the suppression of SF in the highest density environments.

In future work we will probe whether the “downsizing” of star formation in the centers of galaxies is indeed responsible for our observed trends by exploring galaxy populations as a function of stellar mass, together with the local density. Since “downsizing” is concerned with the mass dependence of the SFR history of galaxies, this will allow a more detailed exploration of the origins and likely evolution of the observed variation in the spatially resolved SF in galaxies.

## 7. Appendix A: Calculation of the flux in the pixels

We utilize one of the photometric data products of the SDSS: the fpAtlas images as described in Paper I. These are cutouts from the imaging data in all five bands ( $u, g, r, i, z$ ) of all detected objects in the survey. The photometry in every pixel that belongs to each galaxy of the fpAtlas image (in each passband) needs to be calibrated in order to obtain a measured flux from the counts in that pixel. In this section, we illustrate the steps that need to be taken to do this. The photometric calibration of the Atlas images was done according to the *asinh* magnitude system developed by Lupton et al. (1999) and foreground Galactic extinction is also corrected for. We follow the prescription for the photometric calibration of the imaging data that is given in the SDSS Photometric Flux Calibration web page<sup>8</sup>. We summarize the basic steps below.

We obtain a count rate  $t/t_0$  from the net count  $N_{DN}$  (in “Data Numbers”,  $DN$ ) in each pixel in each of the passbands ( $u, g, r, i, z$ ).

$$\frac{t}{t_0} = \frac{N_{DN} \times 10^{0.4 \times (a_0 + (k \times A))}}{T} \quad (3)$$

where  $t/t_0$  is defined to be the count rate and  $t_0$  is the zero point count rate and is given by  $t_0 = 10^{-0.4 \times a_0}$ .  $T$  is the exposure time of the SDSS 2.5 meter telescope,  $k$  is the atmospheric extinction coefficient in a particular passband and  $A$  is the airmass (optical path length relative to zenith for light travelling through the Earth’s atmosphere) for that

---

<sup>8</sup><http://www.sdss.org/dr4/algorithms/fluxcal.html>

passband.  $a_0$  is the zero-point in each passband.  $k$ ,  $A$  and  $a_0$  are obtained from the `Field` table of the SDSS Catalog Archive Server (CAS, <http://cas.sdss.org/dr4/>). For the  $r'$  band, these correspond to the `kk_r`, `airmass_r` and `aa_r` columns.

The count rate is then converted to an SDSS *asinh* magnitude  $m$  (and thence to an AB flux) using:

$$m = -\frac{2.5 \times (\text{asinh}((t/t_0)/2b) + \ln(b))}{\ln(10)} \quad (4)$$

where  $b$  is a softening parameter for a particular photometric band (`bPrime_r` for the  $r'$  band in CAS). The magnitudes are corrected for foreground Galactic extinction using the values of extinction (in magnitudes) in each band that are found in the `PhotoObjAll` table (`extinction_r` for the the  $r'$  filter). These values are obtained from the maps of foreground dust infrared emission produced by Schlegel et al. (1998).

The error in the counts  $N_{DN}$  is calculated from the Poisson error from the photoelectrons which are counted by the CCD detectors, and the total noise contributed by read noise and dark currents:

$$\delta N_{DN} = \sqrt{\left(\frac{N_{DN} + N_{sky}}{G}\right) + N_{pix} \times (D + \delta N_{sky})} \quad (5)$$

where  $N_{sky}$  is the number of sky counts (in  $DN$ ) over the area considered, obtained from the average sky background level in the frame (in *maggies/arcsec<sup>2</sup>*) that the object was found in, given in the `sky_r` column in the `Field` table for the  $r'$  band.  $N_{pix}$  is the area covered by the object in pixels ( $N_{pix} = 1$  for one pixel).  $D$  is the noise due to dark variance (obtained from the `darkVariance_r` column in the `Field` table for the  $r'$  band) and  $\delta N_{sky}$  is the error on the estimate of the average sky level in the frame (obtained from the `skyErr` column in the `Field` table and then converting *maggies/arcsec<sup>2</sup>* to  $DN/pix$ ).

Finally, we work out the error in the SDSS magnitude (from which we can derive an error in the flux):

$$\delta m = \frac{2.5 \times \delta N_{DN} \times 10^{0.4 \times (a_0 + k \times A)}}{2bT \times \ln(10) \times \sqrt{1 + \left(\frac{t}{2bt_0}\right)^2}} \quad (6)$$

The Point Spread Function (PSF) is not taken into account in our analysis. The median seeing value reported in DR4 was 1.4'' so the PSF will be 3–4 pixels across typically. We have

ignored this effect for now since, as long as the galaxies are sufficiently resolved, there will be useful information to be gained regardless of whether the small-scale details of structure that will be smeared by the PSF can be extracted. Although seeing can indeed affect the innermost annulus in galaxies, for over 53% of galaxies, this annulus ( $r \leq 0.125R_p$ ) is larger in angular scale than the PSF width.

## 8. Acknowledgments

We would like to thank the referee for their valuable input which has improved this paper. NW would like to thank Andrew Zentner, Jeff Newman and Michael Cooper for useful discussions. This material is based upon work supported by the National Science Foundation under Grant No. 0851007 and AST 0806367. AMH acknowledges support provided by the Australian Research Council in the form of a QEII Fellowship (DP0557850). This material is also based upon work supported by the National Science Foundation under the following NSF programs: Partnerships for Advanced Computational Infrastructure, Distributed Terascale Facility (DTF) and Terascale Extensions: Enhancements to the Extensible Terascale Facility.

Funding for the SDSS and SDSS-II has been provided by the Alfred P. Sloan Foundation, the Participating Institutions, the National Science Foundation, the U.S. Department of Energy, the National Aeronautics and Space Administration, the Japanese Monbukagakusho, the Max Planck Society, and the Higher Education Funding Council for England. The SDSS Web Site is <http://www.sdss.org/>. The SDSS is managed by the Astrophysical Research Consortium for the Participating Institutions. The Participating Institutions are the American Museum of Natural History, Astrophysical Institute Potsdam, University of Basel, University of Cambridge, Case Western Reserve University, University of Chicago, Drexel University, Fermilab, the Institute for Advanced Study, the Japan Participation Group, Johns Hopkins University, the Joint Institute for Nuclear Astrophysics, the Kavli Institute for Particle Astrophysics and Cosmology, the Korean Scientist Group, the Chinese Academy of Sciences (LAMOST), Los Alamos National Laboratory, the Max-Planck-Institute for Astronomy (MPIA), the Max-Planck-Institute for Astrophysics (MPA), New Mexico State University, Ohio State University, University of Pittsburgh, University of Portsmouth, Princeton University, the United States Naval Observatory, and the University of Washington.

## REFERENCES

Adelman-McCarthy J. K., et al. 2006, ApJS, 162, 38

- Abraham, R. G., van den Bergh, S., Nair, P. 2003, *ApJ*, 588, 218
- Benson A. J., Frenk C. S., Baugh C. M., Cole S., Lacey C. G., 2001, *MNRAS*, 327, 1041
- Blanton, M. R., et al. 2001, *AJ*, 121, 2358
- Blanton, M. R., et al. 2003, *AJ*, 125, 2348
- Blanton, M. R., et al. 2005, *AJ*, 129, 2562
- Bruzual, G., Charlot, S. 2003, *MNRAS*, 344, 1000
- Butcher, H., Oemler, A., Jr. 1978, *ApJ*, 219, 18
- Byrd, G., Valtonen, M. 1990, *ApJ*, 350, 89
- Cattaneo A., Dekel A., Faber S. M., Guiderdoni B. 2008, arXiv:0801.1673
- Conselice, C. J. 2006, *MNRAS*, 373, 1389
- Conti A., et al. 2003, *AJ*, 126, 2330
- Cooper, M. C., et al. 2006, *MNRAS*, 370, 198
- Cooper, M. C., et al. 2008, *MNRAS*, 383, 1058
- Cowie, L. L., Songaila, A., Hu, E. M., Cohen, J. G. 1996, *AJ*, 112, 839
- de Vaucouleurs, G., et al. 1991, “Third Reference Catalog of Bright Galaxies”, Springer-Verlag, New York
- Diaferio A., Kauffmann G., Balogh M. L., White S. D. M., Schade D., Ellingson E., 2001, *MNRAS*, 323, 999
- Doyle, M. T., Drinkwater, M. J. 2006, *MNRAS*, 372, 977
- Dressler, A., et al. 1997, *ApJ*, 236, 351
- Dressler, A. 1980, *ApJ*, 236, 351
- Driver, S. P., Allen, P. D., Liske, J., Graham, A. W. 2007, *ApJ*, 657, L85
- Elbaz et al. 2007, *A&A*, 468, 33
- Fasno G., Poggianti B. M., Couch W. J., Bettoni D., Kjaergaard P., Moles M., 2000, *ApJ*, 542, 673

- Gómez, P. L., et al. 2003, *ApJ*, 584, 210
- Goto et al. 2003, *MNRAS*, 346, 601
- Gunn, J. E., & Gott, J. R. I. 1972, *ApJ*, 176, 1
- Heavens, A., Panter, B., Jimenez, R., & Dunlop, J. 2004, *Nature*, 428, 625
- Holden et al. 2007, *ApJ*, 670, 190
- Hubble, E. 1936, “The Realm of the Nebulae”, Yale University Press
- Lintott, C. J., et al. 2008, *MNRAS*, 389, 1179
- Lupton, R. H., Gunn, J. E., Szalay, A. S. 1999, *AJ*, 118, 1406
- Juneau, S., et al. 2005, *ApJ*, 619, L135
- Lewis, I., et al. 2002, *MNRAS*, 334, 673
- Moore B., Katz N., Lake, G., Dressler, A., Oemler A., 1996, *Nat*, 379, 613
- Neistein E., van den Bosch F. C., Dekel A. 2006, *MNRAS*, 372, 933
- Panter, B., Heavens, A. F., Jimenez, R. 2004, *MNRAS*, 355, 764
- Park C., Choi Y.-Y. 2005, *ApJ*, 635, 29
- Park C., Choi Y.-Y., Vogeley M. S., Gott J. R. I., Blanton M. R. 2007, *ApJ*, 658, 898
- Patel, S. G., et al. 2008, *MNRAS*, 2008arxiv0812.2021
- Postman, M., Geller, M. J., 1984, *ApJ*, 281,95
- Sandage, A. R. 1961, “The Hubble atlas of galaxies”, Carnegie Institute of Washington, Washington
- Schlegel, D. J., Finkbeiner, D. P., Davis, M. 1998, *ApJ*, 500, 525
- Seymour, N., et al. 2008, *MNRAS*, 386, 1695
- Shimasaku, K., et al. 2001, *AJ*, 122, 1238
- Strateva et al. 2001, *AJ*, 122, 1861
- Tran K. H., Simard L., Zabludoff A. I., Mulchaey J. S., 2001, *ApJ*, 549, 172

van den Bosch, F.C., et al. 2008, MNRAS, 387, 79

van der Wel., et al. 2007, ApJ, 670, 206

Welikala, N., Connolly A. J., Hopkins A. M., Scranton R., Conti A. ApJ, 677, 970

Whitmore B. C., 1995, in Richter O.-G.,orne K.,eds, ASP Conf.Ser. Vol.70, Groups of Galaxies, Astron.Soc.Pac., San Fransisco, p. 41

Yee H. K. C., Ellingson E., Carlberg R. G., 1996, ApJS, 102, 269

York, D. G., et al. 2000, AJ120, 1579

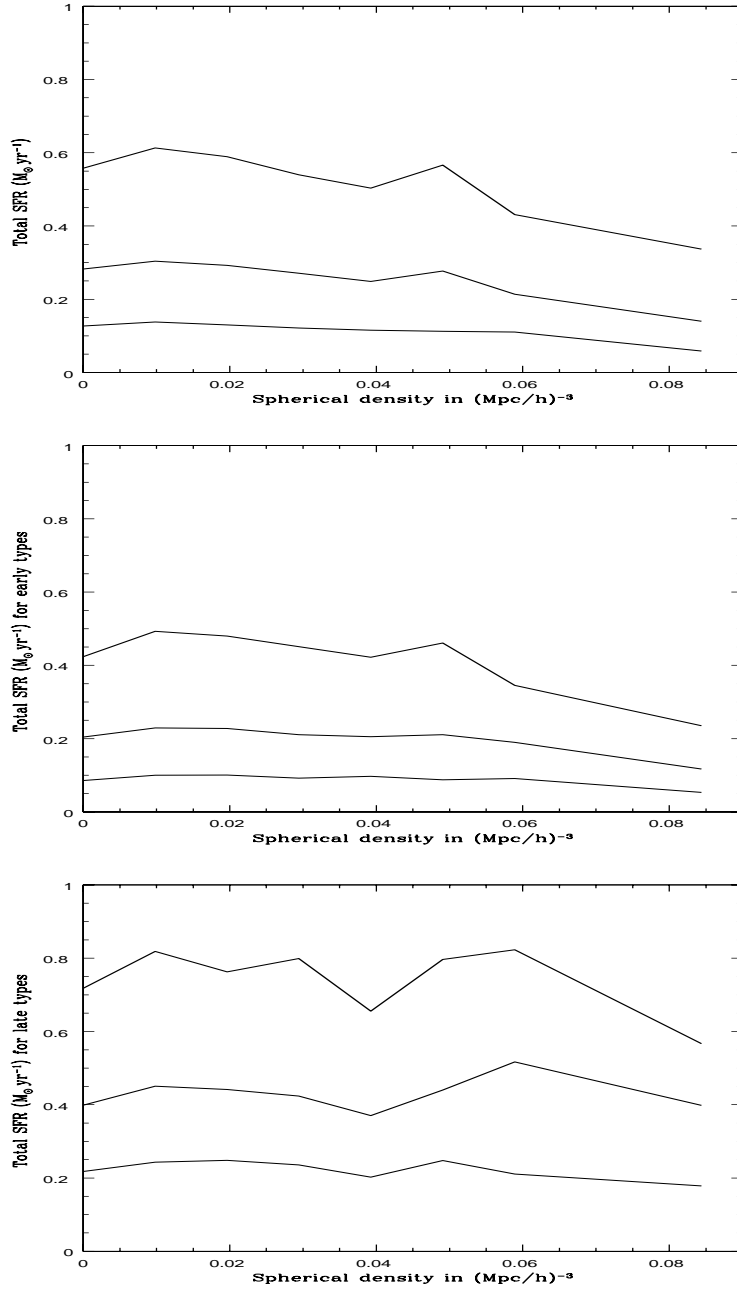


Fig. 1.— Galaxy SFR in  $M_{\odot} \text{ yr}^{-1}$  as a function of density, where the SFR is calculated from a weighted sum over pixels in each galaxy. Top panel: for all types. Middle panel: for early-type galaxies. Bottom panel: for late-type galaxies. Unlike the analysis in Paper I, the spatial extent is constrained to  $1.5 R_p$  within which the SFRs in the pixels of galaxies are counted. The lines indicate the 75th, median and 25th percentiles of the SFR distribution respectively. Late-type galaxies now dominate the tail of the total SFR distribution at all densities. The trends with environment are identical to those found in Paper I, Figure 8 since only a higher fraction of low signal-to-noise and sky pixels are removed here. The decrease at higher densities is most noticeable in the most strongly star-forming galaxies, those in the 75th percentile of the total SFR distribution.



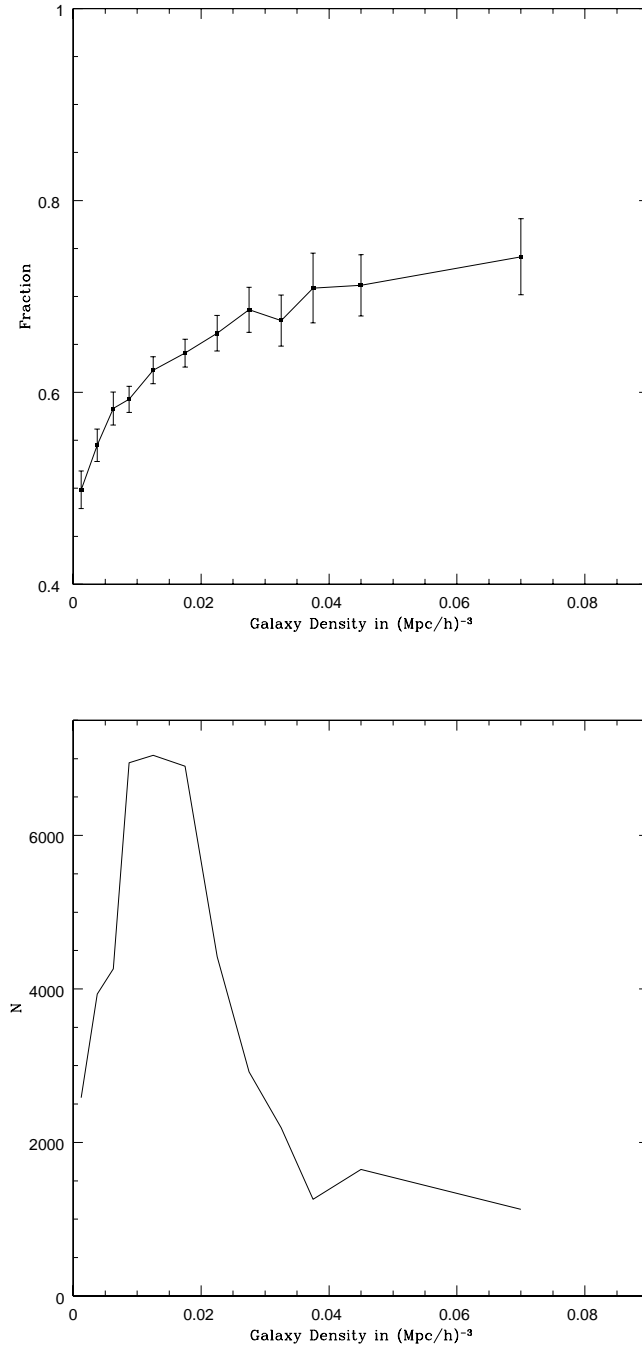


Fig. 2.— Top panel: The density-morphology relation, showing the fraction of early-type galaxies (with  $C_{in} < 0.4$ ). Error bars are Poisson. Bottom panel: Number of galaxies in each interval of local galaxy density. The local galaxy density is sampled more finely in these bins than in the subsequent analysis, where only three intervals of local density are used.

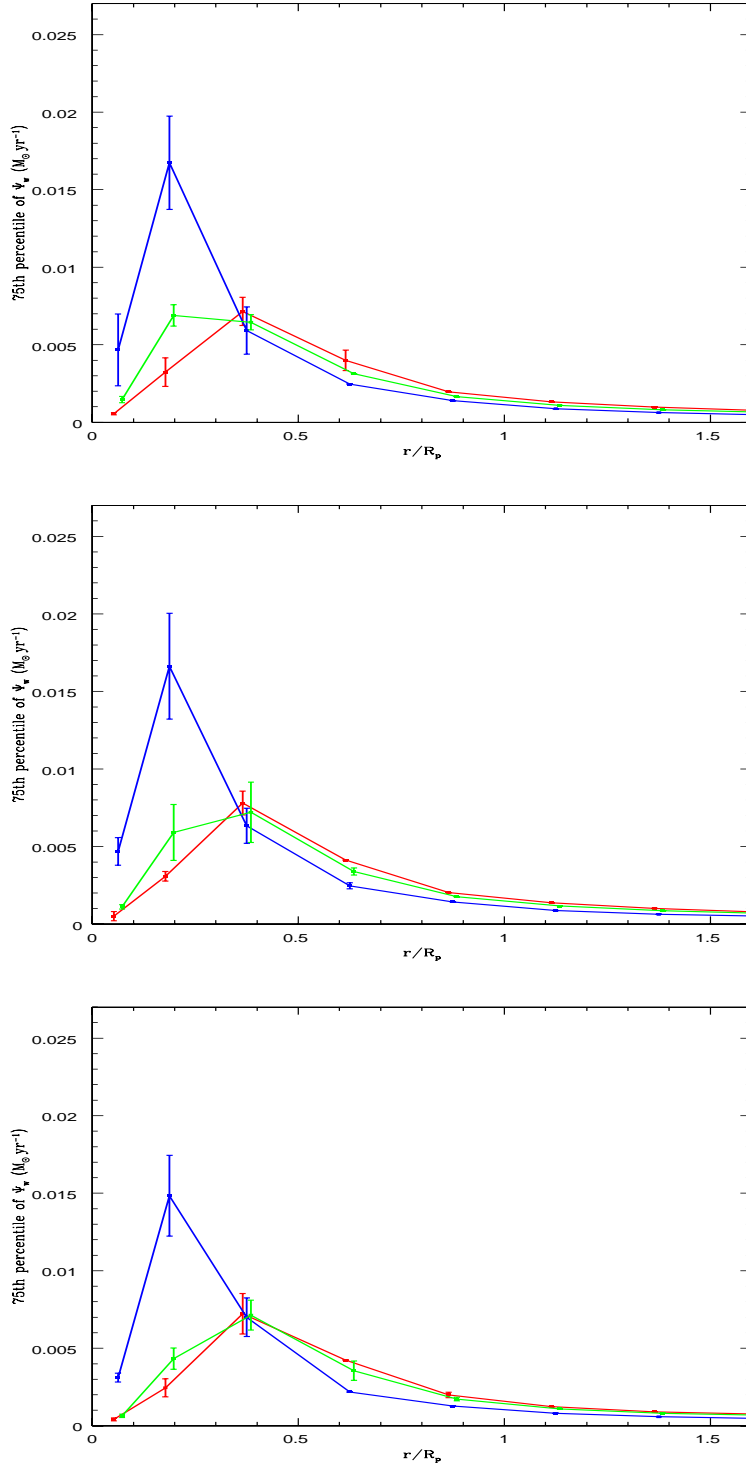


Fig. 3.— Top panel: 75th percentiles of the distribution of weighted mean SFRs  $\Psi_w$  ( $M_\odot \text{yr}^{-1}$ ) within successive radial annuli for early-type galaxies (red), late-type galaxies (blue), and all galaxies (green) which have local galaxy densities  $\rho$  in the range  $0.0 < \rho \leq 0.01 \text{ (Mpc/h)}^{-3}$ . Middle panel:  $0.01 < \rho \leq 0.04 \text{ (Mpc/h)}^{-3}$ . Bottom panel:  $0.04 < \rho \leq 0.09 \text{ (Mpc/h)}^{-3}$ . The three density intervals are the same as those used in Paper I, Figure 9.

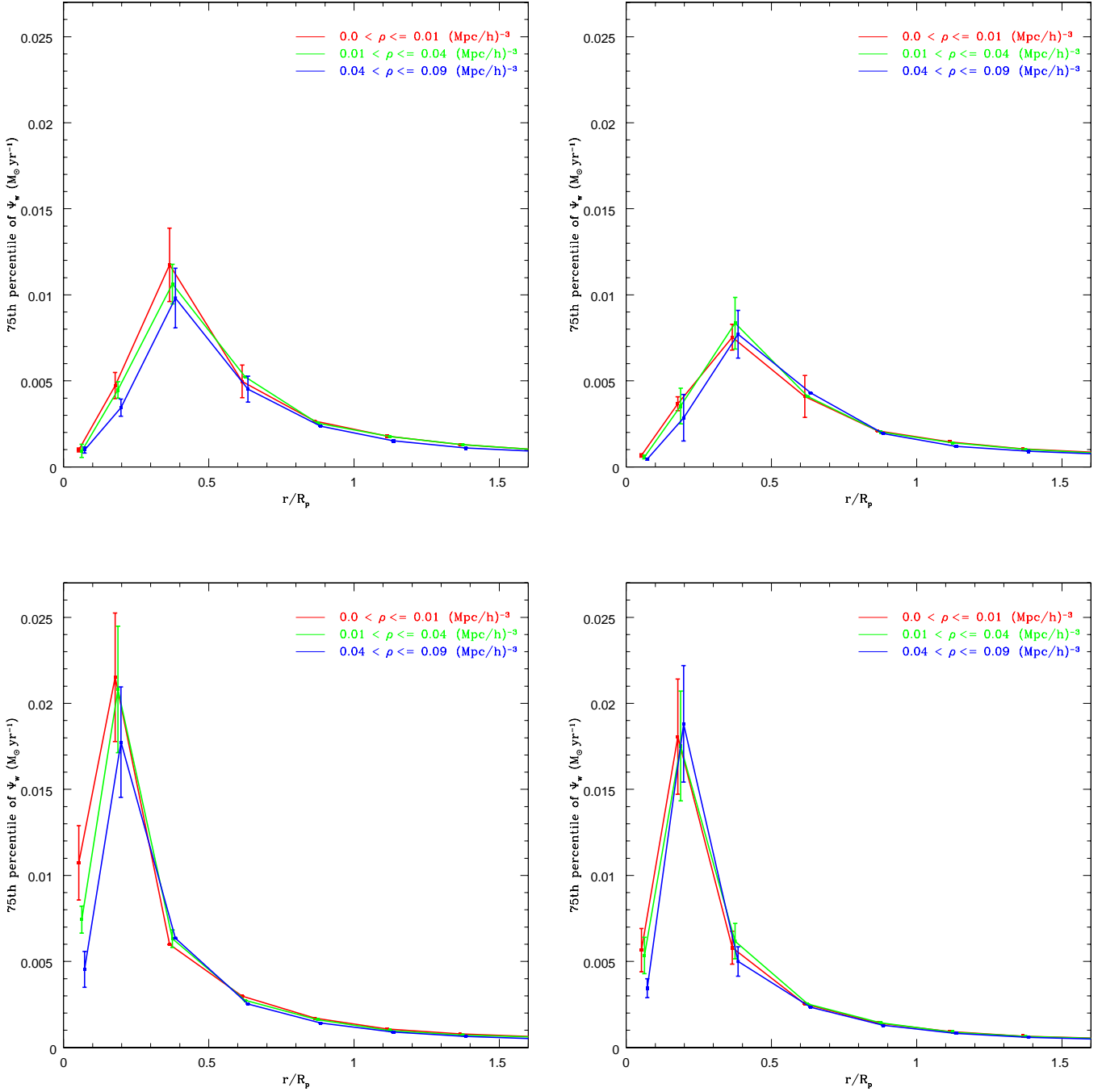


Fig. 4.— 75th percentiles of the distribution of weighted mean SFRs  $\Psi_w$  ( $M_\odot \text{ yr}^{-1}$ ) within successive radial annuli as a function of the local galaxy density  $\rho$  for the highly SF populations of either galaxy type. The intervals of local galaxy density  $\rho$  considered are  $0.0 < \rho \leq 0.01$  ( $\text{Mpc}/h$ ) $^{-3}$  (red),  $0.01 < \rho \leq 0.04$  ( $\text{Mpc}/h$ ) $^{-3}$  (green),  $0.04 - 0.09$  ( $\text{Mpc}/h$ ) $^{-3}$  (blue). Top left panel: For the early-type galaxies in the highest quartile of the total galaxy SFR (‘the highest SF galaxies’). Top right panel: For early-type galaxies in the second highest quartile of the total galaxy SFR (‘the next highest SF galaxies’). Bottom left panel: For the highest SF late-type galaxies. Bottom right panel: For the next highest SF late-type galaxies.

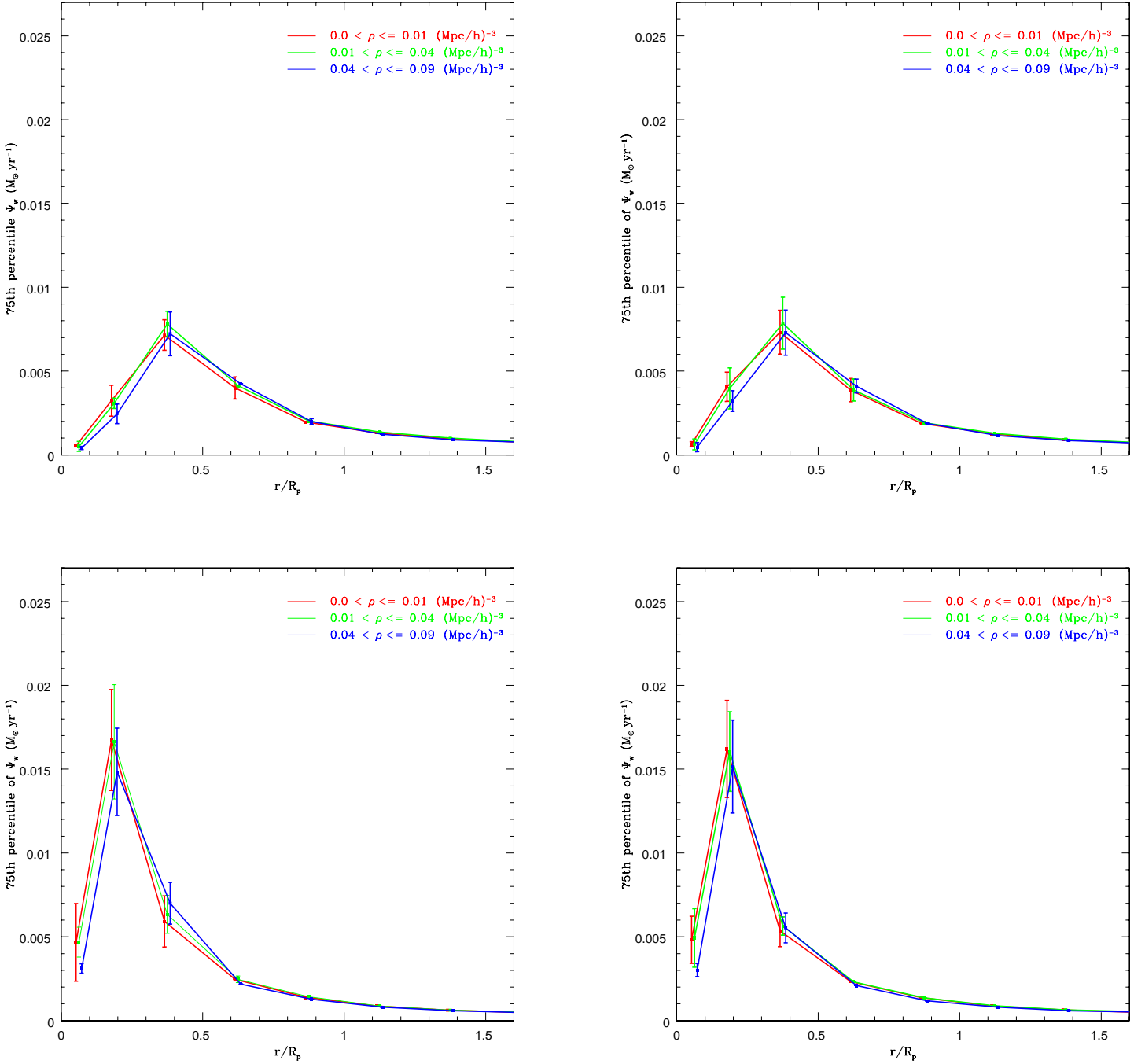


Fig. 5.— 75th percentiles of the distribution of weighted mean SFRs  $\Psi_w$  ( $M_\odot \text{ yr}^{-1}$ ) within successive radial annuli as a function of the local galaxy density  $\rho$  for the full sample of galaxies of either type. No cuts in total SFR are made here. Top left panel: For all early-type galaxies chosen according to the inverse concentration index ( $C_{in} < 0.4$ ). Top right panel: For all early-type galaxies chosen according to the Sersic index ( $n > 2$ ). Bottom left panel: late-type galaxies chosen using  $C_{in} > 0.4$ . Bottom right panel: late-type galaxies chosen using  $n < 2$ .

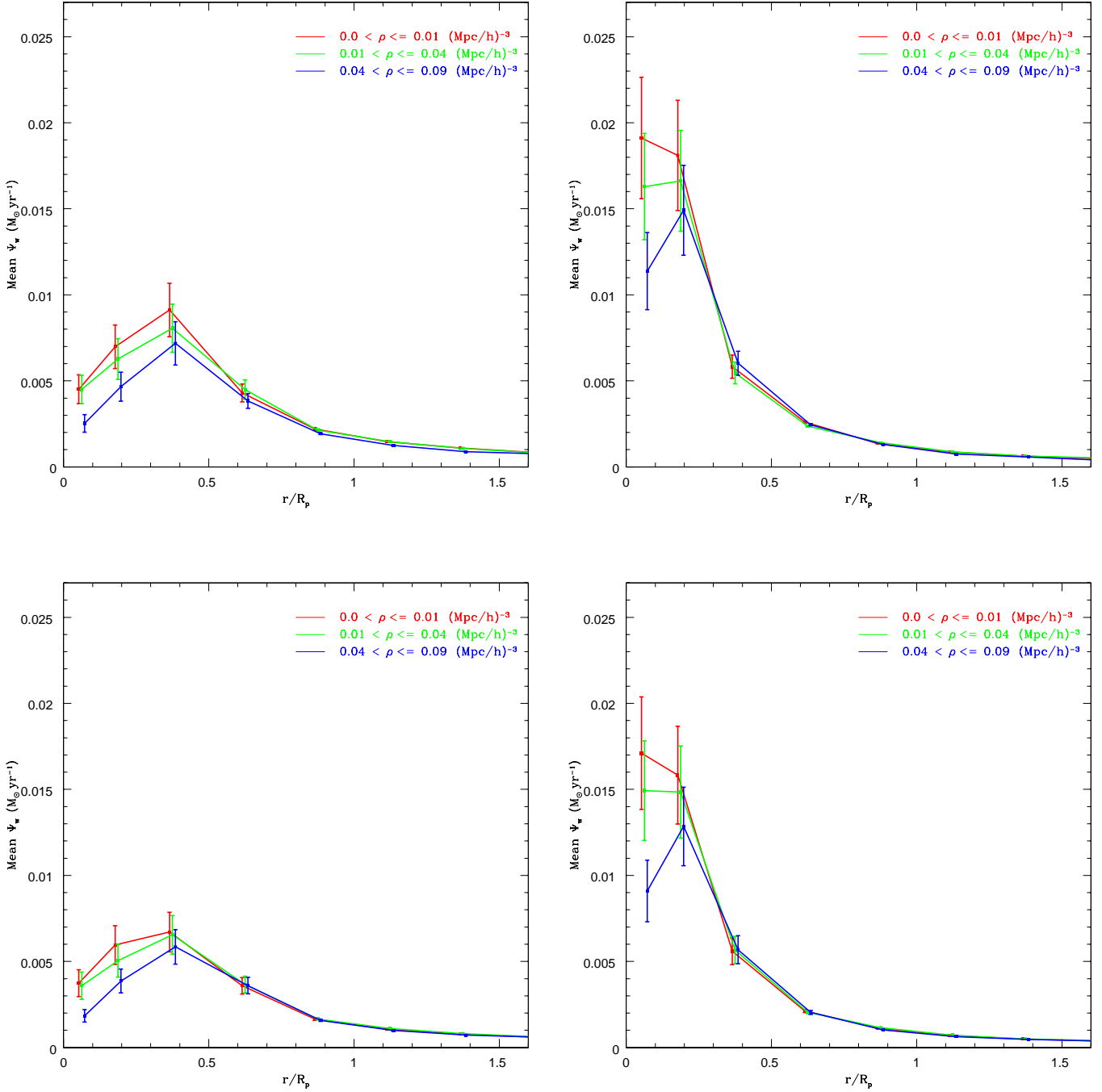


Fig. 6.— Mean of the distribution of weighted mean SFRs  $\Psi_w$  ( $M_\odot \text{ yr}^{-1}$ ) within successive radial annuli as a function of the local galaxy density  $\rho$ . Top left panel: For the highest SF early-type galaxies. Top right: For highest-SF late-type galaxies. Bottom left panel: For all early-types in the full sample (no cuts in the total SFR are made). Top right panel: For all late-type galaxies in the full sample.

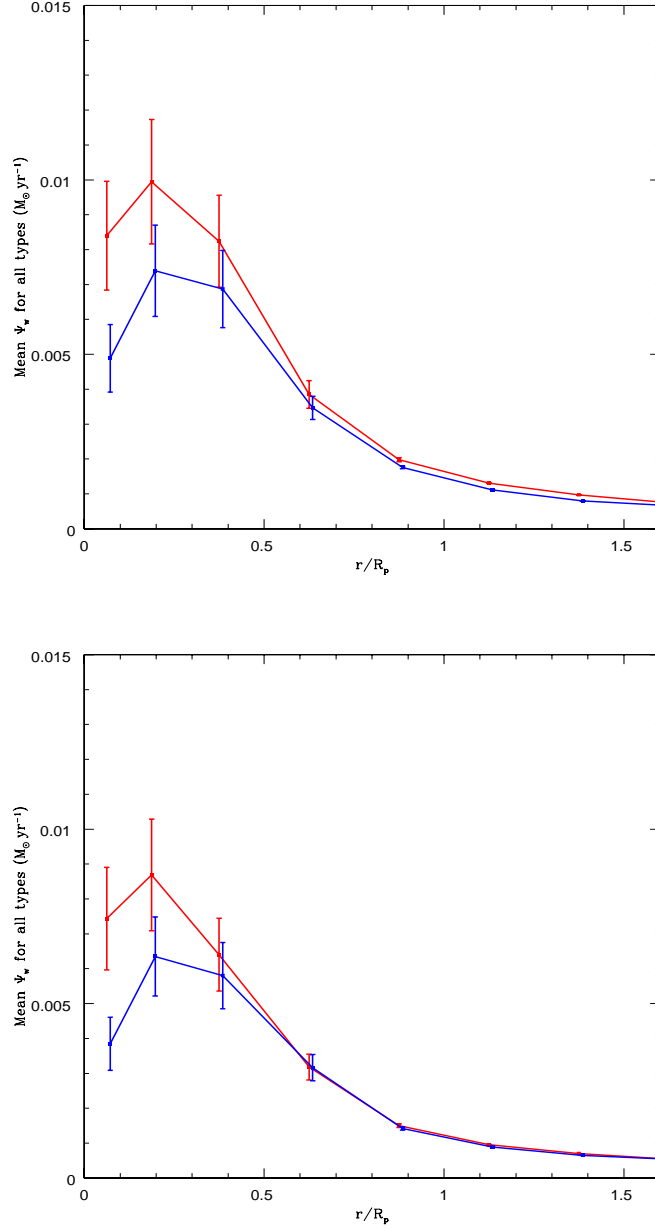


Fig. 7.— The contribution of the density-morphology relation to the observed dependence of SFR on galaxy density. The red line is the artificial composite SFR radial profile (for both early and late-types) in the highest density interval for the highest SF galaxies. The profile is obtained by taking the SFR profiles of the highest SF early and late-types in the lowest density interval, averaging them and weighting by the relative proportion of early and late-types in the highest density environments (see §3.4). This artificial composite profile thus predicts what the SFR profile would look like in the highest density environment if it arose from the density-morphology relation alone. This profile can then be compared to the observed composite profile in the highest density environment (in blue). The bottom panel shows the composite artificial and observed SFR profiles for the full sample of galaxies (not just the highly star-forming ones).

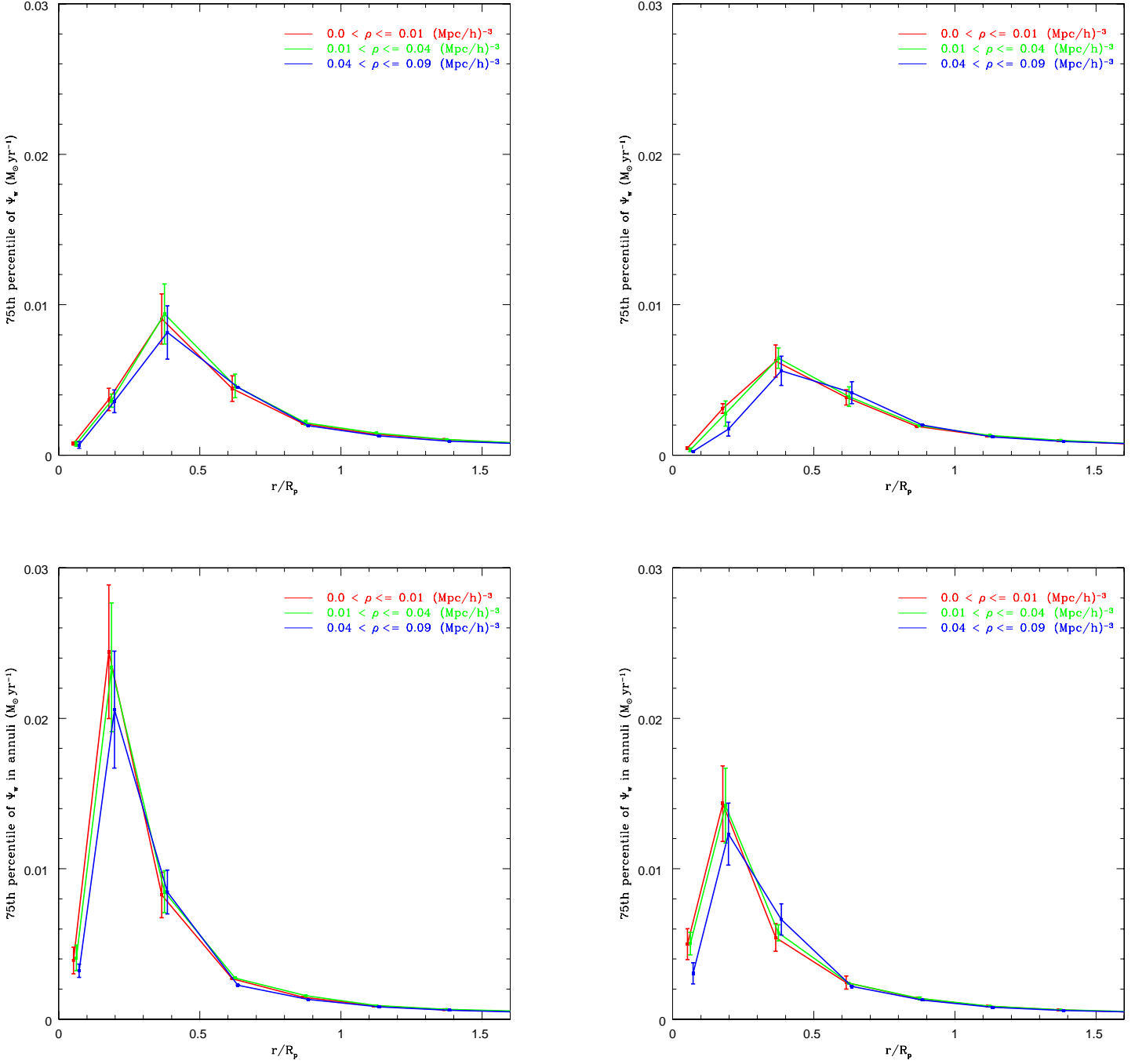


Fig. 8.— Top panel: 75th percentile of the distribution of weighted mean SFRs  $\Psi_w$  ( $M_\odot \text{ yr}^{-1}$ ) within successive radial annuli as a function of the local galaxy density  $\rho$  for early-type galaxies in our sample in intervals of absolute magnitude:  $-22.5 < M_r \leq -21.5$  (top left) and  $-21.5 < M_r \leq -20.5$  (top right). Bottom panel: for late-type galaxies for the same two absolute magnitude intervals.